

Functionalized Polyethyleneimine-gold Nanoparticles-Porphyrin Nanocomposite for Electrochemical Glucose Biosensing

Shumei Gu^{1†}, Kefeng Ma^{1†}, Jinming Kong^{1,*}, Khalid A. Al-Ghanim², Shahid Mahboob², Ying Liu¹ and Xueji Zhang^{3,*}

¹ School of Environmental and Biological Engineering, Nanjing University of Science and Technology, Nanjing 210094, P. R. China

² Department of Zoology, College of Science, King Saud University, P.O. Box 2455, Riyadh-11451, Saudi Arabia

³ Chemistry Department, College of Arts and Sciences, University of South Florida, East Fowler Ave, Tampa, Florida 33620-4202, United States

[†] These authors contributed equally to this work.

*E-mail: j.kong@njust.edu.cn, xueji@usf.edu

Received: 18 March 2017 / Accepted: 24 April 2017 / Published: 12 May 2017

In this work, a novel polyethyleneimine-gold nanoparticles-porphyrin (PEI-AuNPs-Fe^{III}MPIX) nanocomposite was constructed by a simple method to achieve excellent electrochemical properties. Firstly, AuNPs were reduced and stabilized by PEI, and then Fe^{III}MPIX was conjugated to this scaffold through amidation reaction. After that, the nanocomposite was functionalized by 4-mercaptophenylboronic acid (MPBA) through Au-S bond for the determination of glucose. By virtue of high affinity of MPBA for 1, 2-diols of glucose, electrochemical activity of Fe^{III}MPIX and the synergistic effect of PEI-coated AuNPs, this biosensor displayed good sensitivity and selectivity for glucose. The electrochemical response was linearly related to glucose concentration in the range from 10 to 350 μM ($R^2=0.9911$). A low detection limit of 2.16 μM (S/N=3) and a high sensitivity of 13.88 $\mu\text{A mM}^{-1} \text{cm}^{-2}$ was obtained. In addition, this biosensor exhibited excellent anti-interference ability against common interferents such as ascorbic acid (AA), dopamine (DA), alanine (Ala) and proline (Pro), and held satisfactory analytical performance for the determination of glucose in human serum samples, indicating promising practical applications in bioanalysis and clinical diagnosis.

Keywords: Porphyrin; Gold nanoparticle; Polyethyleneimine; 4-Mercaptophenylboronic acid; Glucose sensor

1. INTRODUCTION

Diabetes mellitus is a common chronic disease characterized by excessive blood glucose that has an adverse effect on health. According to the study of World Health Organization, about 180

million people are suffering from this disease, and this number is estimated to be doubled by the year 2030 [1,2]. Considering this, a reliable method for blood glucose concentration monitoring is crucial to the diagnosis and management of diabetes. Various analytical techniques including spectrophotometry [3], chromatographic assay [4], fluorimetric assay [5] and electrochemical sensor [6,7] have been applied in the detection of glucose. Among them, electrochemical sensor exhibits many advantages including high sensitivity and selectivity, fast response, low-cost and convenient operation. For the construction of glucose sensors, boronic acid derivative is a good candidate, owing to its ability to bind with 1, 2-diols of glucose specifically [8,9]. Also, in terms of affinity for glucose, it is superior to glucose oxidase, which is susceptible to various factors such as temperature and pH [10]. Consequently, more and more sensing systems for glucose determination have been fabricated using boronic acid derivatives instead of glucose oxidase.

As known to all, most boronic acid derivatives rarely have electroactivity, thus they are incapable of outputting the signal of the boronic acid-diol binding event [11]. To overcome this obstacle, several researchers added electron mediators into the electrolytes or combined boronic acid derivatives with foreign redox mediators, such as Prussian blue and ferrocene [12,13]. Nevertheless, the redox mediators in the solution would pollute the samples as well as the reference and counter electrodes. Furthermore, the conjunction of redox mediators and boronic acid derivatives is often performed with high reaction temperature, complex steps and harmful organic reagents. Therefore, it is highly desired to explore a facile strategy which is easy to operate, time-saving and environmentally friendly. Herein, Fe^{III}MPIX, a member of porphyrin family, is chosen as an efficient redox signal indicator. Although the catalytic and electrochemical properties of porphyrin have been widely investigated, biomolecule recognition studies based on porphyrin are very limited [14,15]. In this system, it was combined to PEI-AuNPs through amidation without any activation or coupling reagents according to our previous report [16]. Then MPBA, a member of boronic acid derivatives with thiol group, was connected to PEI-AuNPs through Au-S bond [12]. As a result, Fe^{III}MPIX is connected with MPBA indirectly through a simple mixing and stirring procedure, and the signal of the binding event could be monitored.

In recent years, nanomaterials have attracted considerable attention in the field of electrochemical sensing due to their outstanding properties like large surface-to-volume ratio, strong adsorption ability, and good electrical conductivity [17-19]. Gold nanoparticles (AuNPs) are generally considered to be such ideal nanomaterials [20]. Its large surface-to-volume ratio significantly increased the density of the immobilized boronic acid receptors, and the interaction of boronic acid with diol can be improved accordingly by inclusion of nanoparticles. Furthermore, AuNPs have been widely used as effective electron transfer promoters between electroactive center and electrode surface in electrochemical sensing process [21-23]. In this proposed system, it improved the efficiency of electron transfer between Fe^{III}MPIX and electrode surface and greatly enhance the sensitivity of the sensor.

Polyethyleneimine (PEI), a cationic polymer with abundant amines, displays attractive properties including fine robustness, excellent film-forming ability and good biocompatibility, which are vital for the development of electrochemical sensors [24,25]. As reported, it also can be used as reductant and stabilizer for AuNPs formation [26,27]. In a word, this polymer can not only control the

growth and agglomeration of AuNPs, but also bring its attractive properties to it [28]. As a result, the immobilized AuNPs show high stability in electrode surface and serve well as a scaffold for coupling of MPBA.

In this study, a nanocomposite was synthesized with above-mentioned Fe^{III}MPIX, AuNPs, and PEI for sensor applications. It was functionalized by boronic acid receptors for glucose determination. The generated PEI-AuNPs-Fe^{III}MPIX-MPBA on the surface of glassy carbon electrode (GCE) showed favorable linear response toward glucose concentration. Additionally, the fabricated sensor exhibited excellent discrimination performance against endogenous interferents like ascorbic acid (AA), dopamine (DA), alanine (Ala) and proline (Pro). Compared with glucose sensors reported previously [29-31], the as-prepared sensor is promising for practical applications due to its simple preparation process, lower detection limit, excellent selectivity and good stability.

2. EXPERIMENTAL

2.1. Chemicals and reagents

Branched polyethyleneimine (PEI, average Mw ~ 25 kDa), hydrogen tetrachloroaurate (III) tetrahydrate (HAuCl₄·4H₂O), 4-mercaptophenylboronic acid (MPBA), and L-proline (Pro) were all purchased from Sigma-Aldrich (St. Louis, MO). Fe(III) mesoporphyrin IX chloride (Fe^{III}MPIX) was purchased from Frontier Scientific Inc. D-(+)-Glucose (C₆H₁₂O₆) was purchased from Sinopharm Chemical Reagent Co., Ltd. (Shanghai, China). L-Ascorbic acid (AA) was purchased from Xilong Chemical Co. Ltd. (Guangdong, China). Dopamine hydrochloride (DA) was purchased from Aladdin Industrial Inc. (Shanghai, China). L-Alanine (Ala) was purchased from J&K Scientific Ltd. (Beijing, China). Normal human serum was obtained from Shanghai Yiji Industrial Co., Ltd. (Shanghai, China). The 0.1 M phosphate buffer saline (PBS) was prepared by mixing the stock solutions of NaH₂PO₄, Na₂HPO₄ and KCl solutions, and the pH was adjusted by adding 0.1 M HCl or NaOH. Unless stated otherwise, all other chemical reagents were of analytical grade or higher and used without further purification. All aqueous solutions were prepared with ultrapure water (≥ 18.25 M Ω ·cm) from a Millipore Milli-Q water purification system.

2.2. Apparatus

UV-vis absorption spectra were recorded on a UV-3600 UV-vis-NIR spectrophotometer (Shimadzu, Japan). Transmission electron microscopy (TEM) image was obtained with a JEOL JEM-2100 transmission electron microscope at an acceleration voltage of 200 kV. Electrochemical measurements were performed on a CHI 760D electrochemical workstation (Shanghai, China) at room temperature. A conventional three-electrode system was used in the work with a bare or modified glassy carbon electrode (GCE) (3 mm in diameter) as the working electrode, a saturated calomel electrode (SCE) as the reference electrode and a platinum wire as counter electrode, respectively.

2.3. Synthesis and functionalization of PEI-AuNPs-Fe^{III}MPIX nanocomposite

Prior to use, the glassware and magnetic stir bar were thoroughly cleaned with freshly prepared aqua regia, rinsed with ultrapure water, and then oven-dried. The synthesis and functionalization of the PEI-AuNPs-Fe^{III}MPIX nanocomposite is depicted in Figure 1A. Briefly, 1.0 mL PEI was firstly homogenized with 10 mL of 1.215 mM HAuCl₄ solution under vigorous stirring; after incubating at 80 °C for 5.0 min the solution turned into ruby red, which was then cooled to room temperature. Subsequently, 12 mL of 0.1 mM Fe^{III}MPIX (dissolved in DMF) was added into the resulting solution, and the mixture was stirred under room temperature for 1.0 h to obtain the nanocomposite of PEI-AuNPs-Fe^{III}MPIX. After that, 10 mL of 5.0 mM MPBA (dissolved in methanol) was added into the above mixture under mild stirring, followed by stirring under room temperature for 2.0 h. Finally, the obtained mixture was centrifuged at 14,000 rpm for 30 min; after removal of the supernatant the resulting precipitate was redispersed in methanol and stored in a refrigerator at 4 °C for further use.

2.4. Preparation of the glucose biosensor

Firstly, the GCE was successively polished with 0.3 and 0.05 μm alumina slurry until a mirror finish was obtained, and then it was cleaned with ethanol and ultrapure water and dried with nitrogen gas prior to use. The cleaned electrode was modified with the as-prepared PEI-AuNPs-Fe^{III}MPIX-MPBA nanocomposite by drop-casting the latter onto it, and dried at room temperature. The preparation procedure of the electrochemical glucose biosensor is illustrated in Figure 1B.

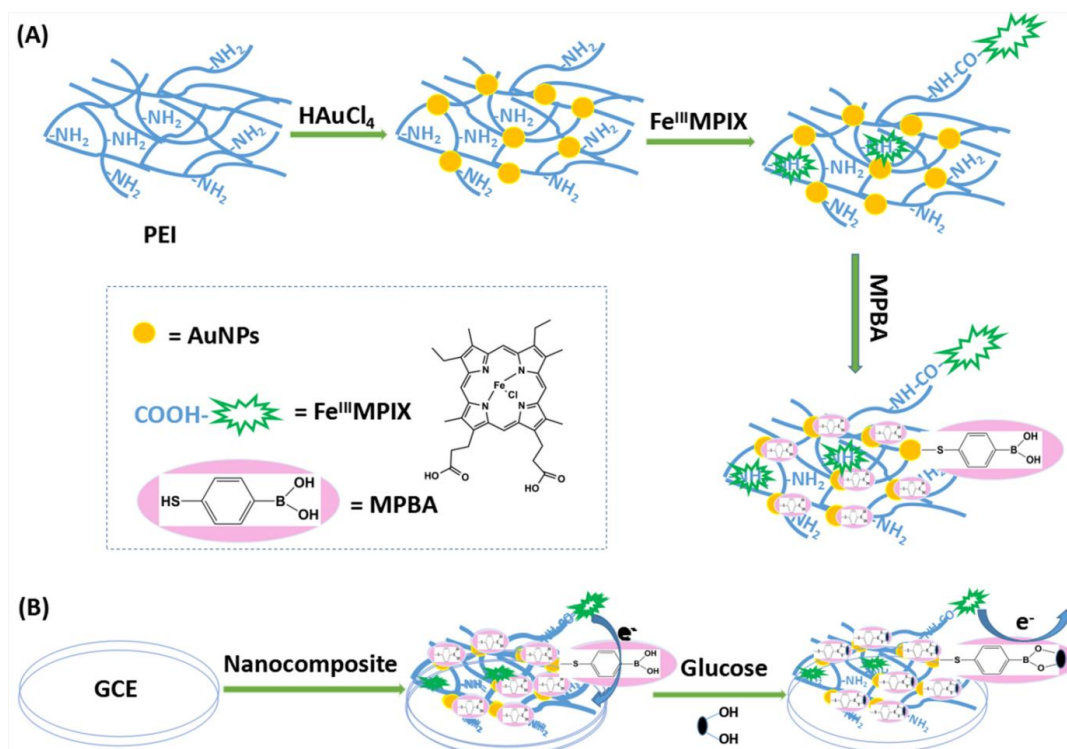


Figure 1. (A) Schematic illustration of the synthesis of the PEI-AuNPs-Fe^{III}MPIX nanocomposite and its functionalization by MPBA. (B) Schematic illustration of the fabrication of the electrochemical glucose biosensor.

3. RESULTS AND DISCUSSION

3.1. UV-vis absorption spectra and TEM Characterizations of the PEI-AuNPs-Fe^{III}MPIX nanocomposite

The successful synthesis of PEI-AuNPs-Fe^{III}MPIX was confirmed by UV-vis absorption spectra. As shown in Figure 2, the solution of Fe^{III}MPIX showed a strong Soret band at 372 nm, and the absorption peaks of PEI-AuNPs nanocomposite were observed at 324 nm and 524 nm, which was corresponding to the absorption of PEI and AuNPs, respectively. The diameter of AuNPs was calculated to be 9.7 nm according to Haiss's theory [32]. After the formation of PEI-AuNPs-Fe^{III}MPIX nanocomposite through amidation, the Soret band of Fe^{III}MPIX exhibited a large red shift of 28 nm, from 372 to 400 nm, and the absorption peak of PEI red shifted from 324 to 348 nm. This is attributed to the electronic conjugation within porphyrin (Fe^{III}MPIX) upon the formation of the PEI-AuNPs-Fe^{III}MPIX conjugate [33,34].

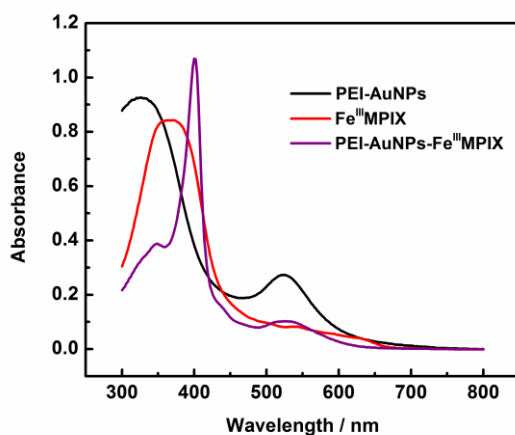


Figure 2. UV-vis absorption spectra of PEI-AuNPs, Fe^{III}MPIX and PEI-AuNPs-Fe^{III}MPIX nanocomposite.

The morphology and size distribution of the PEI-AuNPs-Fe^{III}MPIX nanocomposite were further characterized by TEM, and results are shown in Figure 3. As seen from it, the as-prepared nanoparticles were predominantly spherical in shape with an average diameter of 9.11 nm (250 particles counted), which was in good agreement with the result calculated by UV-vis absorption spectra. Obviously, the AuNPs formed in this way were sparsely and randomly dispersed well on the surface of PEI with uniform structure and similar size. This high monodispersity was owing to the template synthesis function of PEI, which avoided size variations arising from random nucleation and growth phenomena [35]. Furthermore, the cationic charge density and the steric effect of PEI kept the nanoparticles apart and led to stable colloid. Thus, PEI was regarded as a promising material to obtain small sized particles with facile synthesis steps.

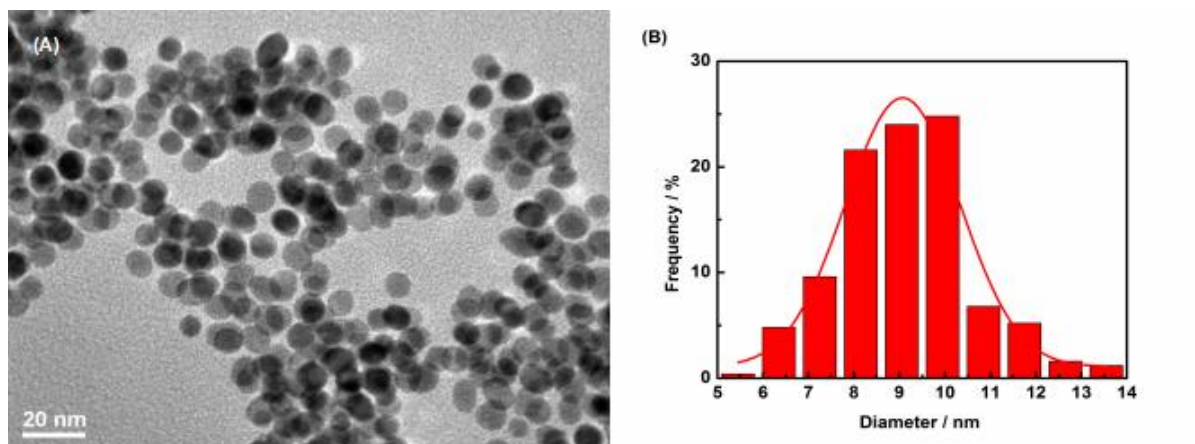


Figure 3. (A) TEM image of the PEI-AuNPs-Fe^{III}MPIX nanocomposite. (B) The size distribution histogram of the immobilized AuNPs.

3.2. Electrochemical characterization of different modified electrodes

In order to further characterize the nanocomposite, electrochemical performance of the modified electrodes in different assembled steps were explored by cyclic voltammetry (CV) in the potential range from -0.8 to 0 V in 0.1 M PBS (pH 8.0). As shown in Figure 4A, there was no electrochemical signal at the bare GCE in the selected potential range. While after the modification of Fe^{III}MPIX, a pair of well-defined redox peaks was observed. The redox peaks can be assigned to the reversible inter-conversion between Fe^{III} and Fe^{II}, which is the typical characteristic of porphyrin modified electrodes according to the previous reports [16,36,37]. In addition, when Fe^{III}MPIX was combined with PEI-AuNPs, a dramatic increase in both redox currents was observed.

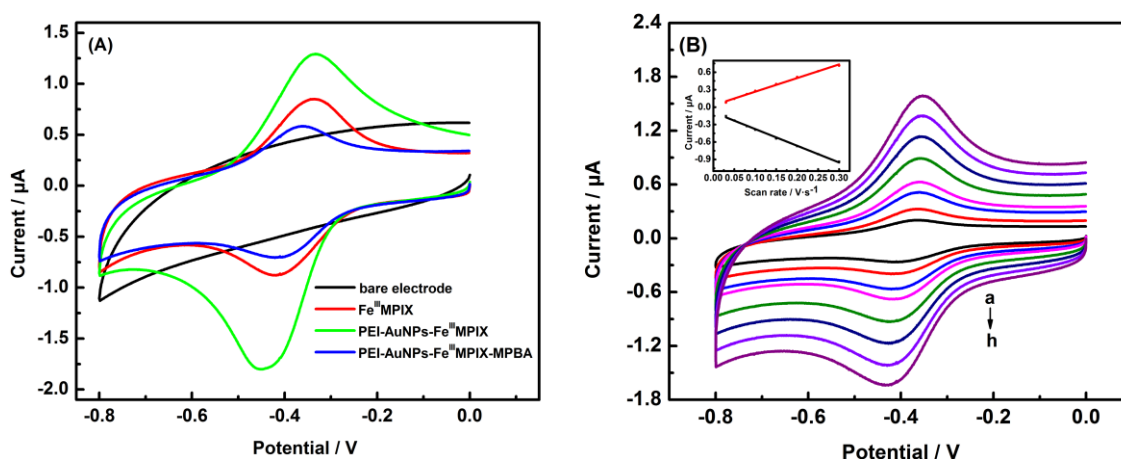


Figure 4. (A) CVs of different modified electrodes in 0.1 M PBS saturated with N₂ (pH 8.0) at a scan rate of 0.1 V s⁻¹. (B) CVs of PEI-AuNPs-Fe^{III}MPIX-MPBA modified electrode in 0.1 M PBS saturated with N₂ (pH 8.0) at different scan rates of (a) 0.03, (b) 0.05, (c) 0.08, (d) 0.1, (e) 0.15, (f) 0.2, (g) 0.25, (h) 0.3 V s⁻¹. (Inset) Plot of redox peak currents versus different scan rates from 0.03 to 0.3 V s⁻¹.

This might be contributed to the loading of small-sized AuNPs that enlarged the exposed surface area and greatly promoted the electron transfer [38,39]. However, after MPBA was assembled on the nanocomposite, the peak currents decreased obviously, suggesting that MPBA hindered the electron transfer [12]. On the basis of this result, we concluded that MPBA was successfully assembled on the PEI-AuNPs-Fe^{III}MPIX nanocomposite.

In addition, we studied the CV responses of PEI-AuNPs-Fe^{III}MPIX-MPBA nanocomposite modified electrode in 0.1 M PBS (pH 8.0) at different scan rates. As shown in Figure 4B, the redox peak potentials changed slightly with the increasing of scan rate. Furthermore, the redox peak currents increased linearly with the scan rate range from 0.03 to 0.3 V s⁻¹. The regression equations could be expressed as i (μA) = 2.3405 v (V s⁻¹) + 0.0314 ($R^2=0.9977$) and i (μA) = -2.8712 v (V s⁻¹)-0.0897 ($R^2=0.9989$), respectively, indicating a surface-controlled electrochemical process [22,40].

3.3. Influence of pH on the sensor response

Different substituent on the phenyl ring of phenylboronic acid allows the pK_a of it to be tuned, normally located between 7.5 and 9.5 as reported in literature [13,41,42]. Additionally, the esterification of phenylboronic acid with glucose is a pH-dependent process, which is similar to the pK_a of the used boronic acid derivatives, so it is necessary to investigate the optimum pH of the reaction. In this work, the electrochemical response of PEI-AuNPs-Fe^{III}MPIX-MPBA modified electrode to glucose was examined by CV in 0.1 M PBS at different pH values. As shown in Figure 5, the peak current decreased obviously when 0.05 mM glucose was added to the solution at pH of 8.0, while the value of current change was negligible at other pH conditions. This revealed that the selected boronic acid derivative in our research interacted with 1, 2-diol of glucose at pH 8.0. The decrease of the current was due to the steric effects caused by the binding of glucose to the immobilized boronic acid moiety, which hindered the access of electron to the electrode surface [43].

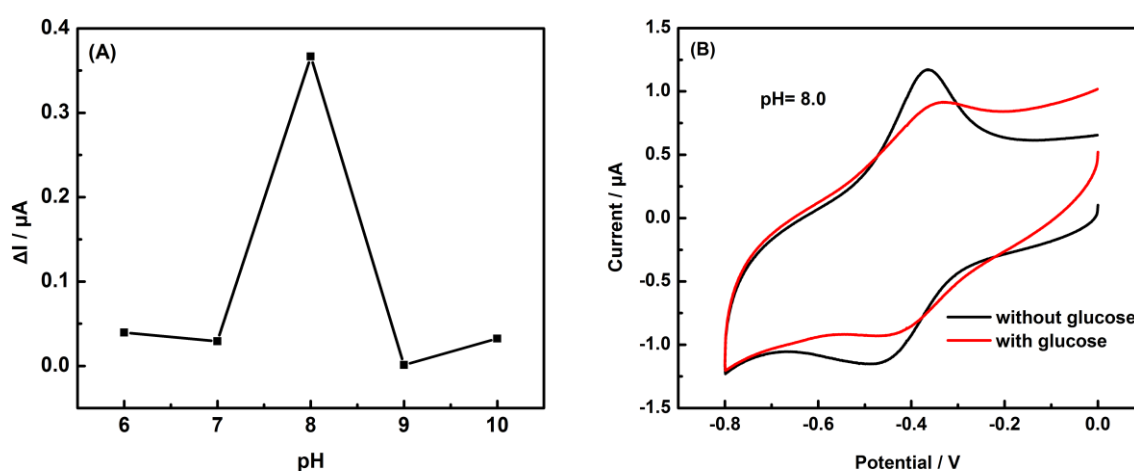


Figure 5. (A) The current change of PEI-AuNPs-Fe^{III}MPIX-MPBA modified electrode in 0.1 M PBS saturated with N₂ at different pH values. $\Delta I = I_1 - I_2$, I_1 : the current of the modified electrode monitored in electrolyte without glucose; I_2 : the current of the modified electrode monitored in electrolyte with 0.05 mM glucose. (B) CVs of PEI-AuNPs-Fe^{III}MPIX-MPBA modified electrode in 0.1 M PBS saturated with N₂ at pH 8.0. Scan rate: 0.1 V s⁻¹.

3.4. Determination of glucose

In the proposed method, the increasing of glucose concentration induced an increase of hindrance and thus a current decrease of the modified electrode. Figure 6A showed DPVs of the PEI-AuNPs-Fe^{III}MPIX-MPBA modified electrode to different concentrations of glucose in 0.1 M PBS. An obvious decrease of the peak current was observed upon successively injecting glucose into the electrolyte. Further, the peak current was found to be proportional to the concentration of glucose and plotted against it from 10 to 350 μM (Figure 6B), suggesting that this novel sensor could successfully read out the boronic acid recognition behavior of glucose at the micromolar levels. The regression equation was expressed as $i (\mu\text{A}) = 9.55525 \times 10^{-4} c (\mu\text{M}) + 0.02849$ with a correlation coefficient of 0.9911. A detection limit of 2.16 μM ($S/N = 3$) was estimated using 3σ . Due to the high conductivity and finely-dispersed recognition sites on the PEI-AuNPs-porphyrin nanocomposite, a sensitivity of $13.88 \mu\text{A mM}^{-1} \text{cm}^{-2}$ and a rapid response within 30 s was achieved.

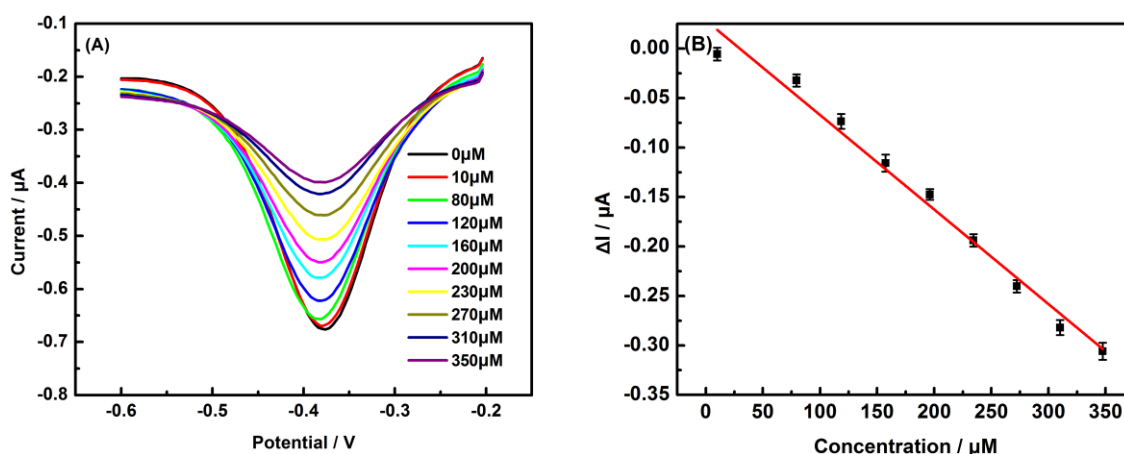


Figure 6. (A) DPVs of PEI-AuNPs-Fe^{III}MPIX-MPBA modified electrode to different concentrations of glucose in 0.1 M PBS saturated with N₂ (pH 8.0). (B) The linear relationship between peak current and glucose concentration.

Table 1. Comparison of our proposed method with other reported electrochemical glucose detection methods based on boronic acid derivatives.

Modified materials	Linear range (mM)	Detection limit (μM)	References
CS*-PDDA*-PB*-AuNPs-MPBA	0.1-1.0; 1.0-100	26	[12]
PBA* bearing redox-polymer	0.02-0.5	7.8	[38]
ABBA*/PSA*/PSSA* fibers-mat	0.75-14	750	[41]
PAPBAOT*	5-50	500	[44]
MWCNTs*-PEI/AuNPs-B(OH) ₂ /GOx*	0.25-5	0.8	[17]
PEI-AuNPs-Fe^{III}MPIX-MPBA	0.01-0.35	2.16	This work

*CS: chitosan; PDDA: poly (diallyldimethylammonium chloride); PB: Prussian blue; PBA: poly (phenol-co-3-hydroxyphenylboronic acid); ABBA: 3-aminobenzene boronic acid; PSA: poly (styrene-co-acrylamide); PSSA: polystyrene sulfonic acid; PAPBAOT: poly (3-aminophenyl boronic acid-co-3-oxylthiophene); MWCNTs: multi-walled carbon nanotubes; GOx: glucose oxidase.

The performances of other electrochemical glucose sensors based on boronic acid derivatives were shown in Table 1. Compared to these reported glucose sensors, the novel PEI-AuNPs-Fe^{III}MPIX-MPBA sensor in this work exhibited linear response to glucose in relatively low concentration with a lower detection limit, indicating a good sensitivity as well as improved analytical performance. In addition, this sensor can be easily prepared under mild conditions without any complicated processes or organic solutions, which are beneficial for practical applications.

3.5. Interference study

To evaluate the anti-interference ability of the PEI-AuNPs-Fe^{III}MPIX-MPBA modified electrode for glucose determination, the interference effects of AA, DA, Ala and Pro, which normally coexist with glucose in human blood serum were examined [34,44,45]. The results of the proposed biosensor with successive addition of interferents into electrolyte were presented in Figure 7. As seen from it, the current decreased obviously when glucose was added to it, while the decrease of current was nearly the same when it was added with any of these interferents. These results showed that glucose can be detected in a mixture of glucose and excess interferents by PEI-AuNPs-Fe^{III}MPIX-MPBA nanocomposite via the specific binding between the immobilized boronic acid group and glucose. The anti-interference ability of the system was attributed to higher binding affinity of glucose that occupied the recognition sites and suppressed other diol molecules like AA and DA. As for Ala and Pro, they were molecules with no diol structure which can't form boronate ester with boronic acid group, thus they have no influence on the detection [38,46].

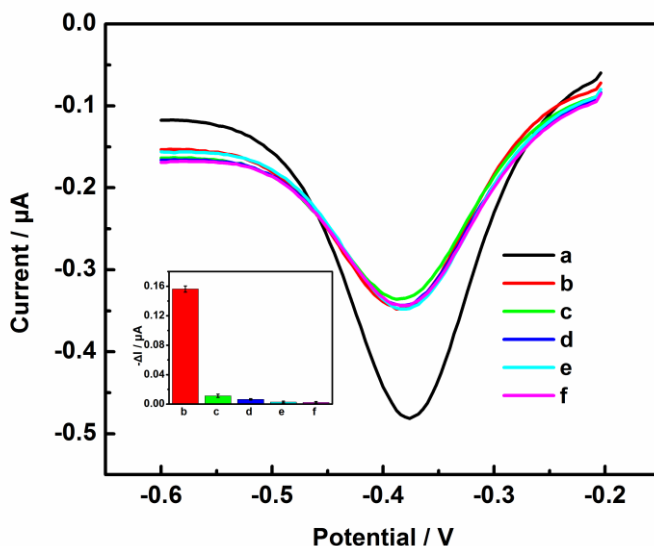


Figure 7. DPVs of PEI-AuNPs-Fe^{III}MPIX-MPBA modified electrode in 0.1 M PBS saturated with N₂ (pH 8.0) containing 0 mM glucose (a), 0.05 mM glucose (b), 0.05 mM glucose + 0.1 mM AA (c), 0.05 mM glucose + 0.1 mM DA (d), 0.05 mM glucose + 0.1 mM Ala (e), 0.05 mM glucose + 0.1 mM Pro (f). (Inset) Current changes caused by glucose and interferents.

3.6. Glucose determination in serum samples

To further demonstrate the feasibility of the novel sensor for real sample analysis, it was applied to detect the concentration of glucose in human serum using the standard addition method [44]. After the sample was diluted 100 times with 0.1 M PBS (pH 8.0), glucose of three different concentration was added into the diluted samples, and the measured current was converted to glucose concentration based on the working curve. As presented in Table 2, the recovery for the determination of glucose was in the range of 97.8-102.4%, indicating that the proposed sensor can be applied to analyze real samples with satisfied results.

Table 2. Determination of glucose in diluted healthy human serum samples (n = 3).

Samples	Add (mM)	Found (mM)	RSD (%)	Recovery (%)
1	0.05	0.0512	2.73	102.4
2	0.08	0.0783	3.14	97.9
3	0.10	0.0978	2.92	97.8

3.7. Reproducibility and stability of the sensor

For the biosensor, reproducibility and stability are also studied as two important parameters [31]. The reproducibility was investigated by measuring the current response of the PEI-AuNPs-Fe^{III}MPIX-MPBA modified electrode to 0.05 mM glucose in 0.1 M PBS (pH 8.0). It showed a repeatability with a relative standard deviation (RSD) of 2.7% for 5 successive assays. In addition, a RSD of 3.1% was obtained for five biosensors prepared independently by the same procedure, further indicating good reproducibility of the sensor. The storage stability of the biosensor was investigated by intermittently measurement in 0.1 M PBS containing 0.05 mM glucose. The current response was remained 99.3% of its initial response in the first week and still remained 92.1% after a month, suggesting excellent stability of the modified electrode. These good properties may be attributed to the immobilization and stabilization effect of PEI-AuNPs scaffold for Fe^{III}MPIX and MPBA, which dramatically enhanced the stability of the sensing platform [40].

4. CONCLUSIONS

In summary, a novel nanocomposite PEI-AuNPs-Fe^{III}MPIX was successfully constructed and functionalized by MPBA to fabricate an electrochemical sensor for glucose. The resulting system exhibited an excellent glucose recognition function ranging from 10 to 350 μ M with a low detection limit of 2.16 μ M. This outstanding performance of outputting the boronic acid-diol binding event was contributed to the superb electrochemical activity of Fe^{III}MPIX and the synergistic effect of PEI-coated AuNPs. Furthermore, the PEI-AuNPs-porphyrin-MPBA nanocomposite was obtained through facile steps and the composite-modified electrode was constructed through a simple casting method. This novel sensor has been applied for the determination of glucose in human serum samples, and the response is in the ideal range, which implies its great potential for practical applications.

ACKNOWLEDGEMENTS

We are grateful to the National Natural Science Foundation of China (21575066 and 1120589) for funding this project.

References

1. J. E. Shaw, R. A. Sicree and P. Z. Zimmet, *Diabetes Res. Clin. Pract.*, 87 (2010) 4.
2. M. Bopp, U. Zellweger and D. Faeh, *Diabetes Care*, 34 (2011) 2387.
3. W. I. Kanchana, T. Sakai, N. Teshima, S. Katoh and K. Grudpan, *Anal. Chim. Acta*, 604 (2007) 139.
4. A. Caseiro, I. L. Marr, M. Claeys, A. Kasper-Giebl, H. Puxbaum and C. A. Pio, *J. Chromatogr. A*, 1171 (2007) 37.
5. P. Shen and Y. Xia, *Anal. Chem.*, 86 (2014) 5323.
6. P. R. Dalmasso, M. L. Pedano and G. A. Rivas, *Biosens. Bioelectron.*, 39 (2013) 76.
7. Y. Gao, T. Yang, X. Yang, Y. Zhang, B. Xiao, J. Hong, N. Sheibani, H. Ghourchian, T. Hong and A. A. Moosavi-Movahedi, *Biosens. Bioelectron.*, 60 (2014) 30.
8. A. Endo, H. Minesaka, T. Hashimoto and T. Hayashita, *Anal. Methods*, 4 (2012) 2657.
9. Q. Wang, L. Yang, X. Yang, K. Wang and J. Liu, *Analyst*, 138 (2013) 5146.
10. F. Li, Z. Wang and Y. Feng, *Sci. China Ser. B: Chem.*, 52 (2009) 2269.
11. Y. Egawa, T. Seki, S. Takahashi and J. Anzai, *Mater. Sci. Eng. C*, 31 (2011) 1257.
12. X. Z. Bian, H. Q. Luo and N. B. Li, *Bioprocess Biosyst. Eng.*, 33 (2010) 971.
13. J. Li, Z. Wang, P. Li, N. Zong and N. Li, *Sens. Actuators B: Chem.*, 161 (2012) 832.
14. R. Kubota, S. Asayama and H. Kawakami, *Chem. Commun.*, 50 (2014) 15909.
15. Y. Zheng, Y. Yuan, Y. Chai and R. Yuan, *Biosens. Bioelectron.*, 79 (2016) 86.
16. J. Kong, X. Yu, W. Hu, Q. Hu, S. Shui, L. Li, X. Han, H. Xie, X. Zhang and T. Wang, *Analyst*, 140 (2015) 7792.
17. M. Eguílaz, R. Villalonga, J. M. Pingarrón, N. F. Ferreyra and G. A. Rivas, *Sens. Actuators B: Chem.*, 216 (2015) 629.
18. M. Liu, R. Liu and W. Chen, *Biosens. Bioelectron.*, 45 (2013) 206.
19. Y. Xia, W. Huang, J. Zheng, Z. Niu and Z. Li, *Biosens. Bioelectron.*, 26 (2011) 3555.
20. C. Wang, J. Qian, K. Wang, X. Yang, Q. Liu, N. Hao, C. Wang, X. Dong and X. Huang, *Biosens. Bioelectron.*, 77 (2016) 1183.
21. D. Brondani, B. De Souza, B. S. Souza, A. Neves and I. C. Vieira, *Biosens. Bioelectron.*, 42 (2013) 242.
22. Y. Chen, Y. Li, D. Sun, D. Tian, J. Zhang and J. J. Zhu, *J. Mater. Chem.*, 21 (2011) 7604.
23. Y. Yu, Z. Chen, S. He, B. Zhang, X. Li and M. Yao, *Biosens. Bioelectron.*, 52 (2014) 147.
24. L. Jin, X. Gao, L. Wang, Q. Wu, Z. Chen and X. Lin, *J. Electroanal. Chem.*, 692 (2013) 1.
25. S. Zhang, A. Bao, T. Sun, E. Wang and J. Wang, *Biosens. Bioelectron.*, 63 (2015) 287.
26. X. Fang, H. Ma, S. Xiao, M. Shen, R. Guo, X. Cao and X. Shi, *J. Mater. Chem.*, 21 (2011) 4493.
27. P. Veerakumar, M. Velayudham, K. L. Lu and S. Rajagopal, *Appl. Catal. A: Gen.*, 455 (2013) 247.
28. K. Kim, H. B. Lee, J. W. Lee, H. K. Park and K. S. Shin, *Langmuir*, 24 (2008) 7178.
29. C. Chen, Y. Fu, C. Xiang, Q. Xie, Q. Zhang, Y. Su, L. Wang and S. Yao, *Biosens. Bioelectron.*, 24 (2009) 2726.
30. S. Liu, J. Tian, L. Wang, Y. Luo, W. Lu and X. Sun, *Biosens. Bioelectron.*, 26 (2011) 4491.
31. B. Unnikrishnan, S. Palanisamy and S. Chen, *Biosens. Bioelectron.*, 39 (2013) 70.
32. W. Haiss, N. T. Thanh, J. Aveyard and D. G. Fernig, *Anal. Chem.*, 79 (2007) 4215.
33. J. Chen, L. Zhao, H. Bai and G. Shi, *J. Electroanal. Chem.*, 657 (2011) 34.
34. C. Shan, H. Yang, D. Han, Q. Zhang, A. Ivaska and L. Niu, *Biosens. Bioelectron.*, 25 (2010) 1070.

35. Y. Kim, S. Oh and R. M. Crooks, *Chem. Mater.*, 16 (2004) 167.
36. S. Zhang, S. Tang, J. Lei, H. Dong and H. Ju, *J. Electroanal. Chem.*, 656 (2011) 285.
37. X. H. Yu, J. M. Kong, X. J. Han and X. J. Zhang, *RSC Adv.*, 4 (2014) 46980.
38. J. Li, L. Liu, P. Wang, Y. Yang and Y. Zheng, *Sens. Actuators B: Chem.*, 198 (2014) 219.
39. C. Wang, S. Chen, Y. Xiang, W. Li, X. Zhong, X. Che and J. Li, *J. Mol. Catal. B: Enzym.*, 69 (2011) 1.
40. J. Chen, W. Zhang and J. Ye, *Electrochem. Commun.*, 10 (2008) 1268.
41. A. Tiwari, D. Terada, C. Yoshikawa and H. Kobayashi, *Talanta*, 82 (2010) 1725.
42. J. N. Cambre and B. S. Sumerlin, *Polymer*, 52 (2011) 4631.
43. H. C. Wang, H. Zhou, B. Chen, P. M. Mendes, J. S. Fossey, T. D. James and Y. T. Long, *Analyst*, 138 (2013) 7146.
44. H. Çiftçi, U. Tamer, M. Ş. Teker and N. Ö. Pekmez, *Electrochim. Acta*, 90 (2013) 358.
45. J. Qiu, J. Huang and R. Liang, *Sens. Actuators B: Chem.*, 160 (2011) 287.
46. L. Liu, N. Xia, Y. Xing and D. H. Deng, *Int. J. Electrochem. Sci.*, 8 (2013) 11161.

© 2017 The Authors. Published by ESG (www.electrochemsci.org). This article is an open access article distributed under the terms and conditions of the Creative Commons Attribution license (<http://creativecommons.org/licenses/by/4.0/>).